Electronic Supplementary Information

Hydration and counterion binding of aqueous acetylcholine chloride and carbamoylcholine chloride

Sergej Friesen,[a] Marina V. Fedotova,[b] Sergey E. Kruchinin,[b] Marija Bešter-Rogač,[c] Črtomir Podlipnik,[c] and Richard Buchner*[a]

---

[a] *Institut für Physikalische und Theoretische Chemie, Universität Regensburg, 93040 Regensburg, Germany. Richard.Buchner@chemie.uni-regensburg.de*

[b] *G.A. Krestov Institute of Solution Chemistry, Russian Academy of Sciences, Akademicheskaya st. 1, 153045 Ivanovo, Russian Federation. E-mail: hebrus@mail.ru*

[c] *Faculty of Chemistry and Chemical Technology, Večna pot 113, University of Ljubljana, SI-1000 Ljubljana, Slovenia. E-mail: marija.bester@fkkt.uni-lj.si*

Dilute-solution conductivity measurements

Measurements of the electrical conductivity, κ, were performed with a precision LCR Meter (Agilent 4284) connected to a three-electrode cell immersed in a thermostat with 3 mK temperature stability.[1] After correction for lead resistance, the obtained conductivities, $\kappa'(\nu)$, recorded in the frequency range $500 \leq \nu/\mathrm{Hz} \leq 10000$, were extrapolated to infinite frequency to eliminate electrode polarization effects and the result, $\kappa = \lim_{\nu\to\infty} \kappa'(\nu)$, converted to molar conductivities, $\Lambda = \kappa/c$ of relative standard uncertainty $u_\mathrm{r}(\Lambda) = 0.0005$ (Tables S5 and S6). Solution densities, ρ, required for converting solute molality m [in $\mathrm{mol\,kg_{solvent}^{-1}}$] to molar concentration, c [in $\mathrm{mol\,L^{-1}} \equiv \mathrm{M}$] at given T were calculated as $\rho(m,T) = \rho(0,T) + b \times m$, using literature data,[2] $\rho(0,T)$, for pure water and density gradients, $b = \mathrm{d}\rho/\mathrm{d}m$ (Tables S5 and S6), obtained at 298.15 K with a vibrating tube densimeter (DMA 5000 M, Anton Paar, Austria).

The $\Lambda(c)$ values of Tables S5 (AChCl(aq)) and S6 (CChCl(aq)) were analyzed with Barthel's low-concentration chemical model (lcCM)[3] where the equations

$$\frac{\Lambda}{\alpha} = \Lambda^\infty - S\sqrt{\alpha c} + E\alpha c \times \ln(\alpha c) + J_1 \alpha c - J_2 \times (\alpha c)^{3/2} \tag{S1}$$

and

$$K_\mathrm{A}^\circ = \frac{1-\alpha}{\alpha^2 c (y'_\pm)^2} \tag{S2}$$

with

$$y'_\pm = \exp(-\frac{\kappa_\mathrm{D} q}{1+\kappa_\mathrm{D} R_{ij}})\,; \qquad \kappa_\mathrm{D}^2 = 16\pi N_\mathrm{A} q \alpha c\,; \qquad q = \frac{e^2}{8\pi\varepsilon_0 \varepsilon k_\mathrm{B} T} \tag{S3}$$

were iteratively solved to yield the limiting molar conductivity, Λ^∞, and the standard-state ion association constant, K_A°, at $c \to 0$. In eqns (S1-S3) the quantity $(1-\alpha)$ is the adjusted fraction of cations and anions forming ion pairs, e the proton charge, ε the static relative permittivity of the solvent, T the Kelvin temperature; k_B and N_A are the Boltzmann and Avogadro constants; ε_0 is the vacuum permittivity.

Expressions for the coefficients S, E, J_1 and J_2 of eq S1 are given in Ref. 3. Whilst S and E are fully defined by the known[4] values for density, ρ_s, viscosity, η and static relative permittivity, ε, of neat water, coefficients J_1 and J_2 are functions of the maximum mutual distance, R_{ij}, up to which anions and cations are counted as ion pairs. In the lcCM model two oppositely charged ions are assumed to form an ion pair if their mutual separation, r, is within $a \leq r \leq R_{ij}$, where $a = r_+ + r_-$ is the contact distance. For the chloride ion $r_- = 0.181\,\mathrm{nm}$[5] was taken, whereas for $\mathrm{ACh^+}$ and $\mathrm{CCh^+}$ an effective radius equal to that of the tetramethylammonium ion, $r_+ = 0.280\,\mathrm{nm}$,[5] was assumed. Accounting for the possible presence of contact (CIP) and solvent-shared (SIP) ion pairs, the upper limit was taken as $R_{ij} = a + 2d_\mathrm{w}$, with $d_\mathrm{w} = 0.28\,\mathrm{nm}$ as the diameter of a water molecule. The obtained fits are shown in Fig. S1; the obtained values for Λ^∞ and K_A° are summarized in Table 1 of the Main Manuscript.

From $\Lambda^\infty(T)$ the limiting ionic conductivities, $\lambda_+^\infty(T) = \Lambda^\infty(T) - \lambda_-^\infty(T)$, of $\mathrm{ACh^+}$ and $\mathrm{CCh^+}$ were calculated using the data of Harned and Owen[6] for $\mathrm{Cl^-}$ (Table S7). The associated self-diffusion coefficients,

$$D_+^\infty = (RT\lambda_+^\infty)/(|z_+|F^2) \tag{S4}$$

where F is the Faraday constant and $z_+ = 1$, as well as Stokes radii,

$$r_{h+} = (|z_+|F^2)/(6\pi N_\mathrm{A}\eta\lambda_+^\infty) \tag{S5}$$

are also given in Table S7.

Dielectric relaxation spectroscopy

Dielectric spectra, $\hat{\eta}(\nu) = \hat{\varepsilon}(\nu) - \mathrm{i}\kappa/(2\pi\nu\varepsilon_0) = \varepsilon'(\nu) - \mathrm{i}[\varepsilon''(\nu) + \kappa/(2\pi\nu\varepsilon_0)]$, were recorded using a home-made waveguide interferometer (IFM) covering 60 - 89 GHz[7] and a coaxial-line reflectometer setup consisting of a 10 MHz to 50 GHz vector network analyzer (VNA, Agilent E8364B) with electronic calibration module (ECal, Agilent N4693A) and commercial open-ended coaxial-line probes optimized for lower (Agilent 85070E-020; nominally 0.2 - 20 GHz) and higher frequencies (Agilent 85070E-050, 1 - 50 GHz).[8] With both VNA probes data were recorded between 50 MHz and 50 GHz for 91 points equidistant on a $\log \nu$ scale. For every sample at least two measurements with independent calibrations were performed with each probe and separately averaged. Primary calibration standards were air (open line), purified mercury (short) and water (load); internal standards for the additional Padé calibration[9] were formamide, propylene carbonate and dimethylacetamide. After correction for dc conductivity, κ, the resulting averaged 50 MHz to 50 GHz data sets for each probe and the IFM data were then concatenated, trimmed if necessary and averaged in the overlapping frequency range to yield the final spectra of $\varepsilon'(\nu)$ and $\varepsilon''(\nu)$ displayed in Figs. S2 & S3.

Conceivable relaxation models

$$\hat{\varepsilon}(\nu) = \sum_{j=1}^{n} \frac{S_j}{[1 + (\mathrm{i}2\pi\nu\tau_j)^{1-\alpha_j}]^{\beta_j}} + \varepsilon_\infty \tag{S6}$$

based on sums of n individual modes j were simultaneously fit to the thus obtained $\varepsilon'(\nu)$ and $\varepsilon''(\nu)$.[10] The individual relaxations j, of amplitude S_j, and relaxation time, τ_j were modelled by the Havriliak-Negami (HN) equation (width parameters $0 \leq \alpha_j < 1$ and $0 < \beta_j \leq 1$) or simplified variants (Cole-Davidson: CD, $\alpha_j = 0$; Cole-Cole: CC, $\beta_j = 1$; Debye: D, $\alpha_j = 0$, $\beta_j = 1$); $\varepsilon_\infty = \lim_{\nu\to\infty} \varepsilon'(\nu)$ is the limiting high-frequency permittivity and $\varepsilon = \varepsilon_\infty + \sum S_j$ the static relative permittivity of the sample.[11] All reasonable models with $n \leq 5$ were tested and the obtained fits and their parameters scrutinized according to the criteria discussed in detail elsewhere.[12] At room temperature all spectra for AChCl(aq) and CChCl(aq) were best fit by sums of four Debye equations (the 4D model, Tables S10 & S11). For reasons explained in the Main Manuscript from low to high frequencies the resolved modes are numbered from one to four in the case of AChCl(aq) and from zero to three for CChCl(aq). Best fits for the AChCl(aq) spectra recorded as a function of temperature changed from 4D at low T via D+CC+D to 3D at high T with modes $j = 2$ and 3 merging (Table S12). In all fits of AChCl(aq) spectra (Tables S10 & S12) ε_∞ and partly also τ_4 were fixed to the value of neat water.[13]

Calculation details

In order to determine the most probable minimum energy conformations of ACh^+ and CCh^+ in water, first Monte Carlo/Stochastic Dynamics (MC/SD) calculations using the OPLSA-2005 force field with implicit water model were performed.[14] Clustering analysis of the 100 conformations sampled for each cation yielded the input for subsequent DFT calculations (B3LYP density functional with 6-31++G** basis set) with the Poisson-Boltzmann finite element (PBF) method as implemented in Jaguar (Schrödinger Suite 2017-3) to account for solvation.[15–18] For both cations their trans-trans (TT) and trans-gauche (TG) conformers (Figs. 1c & d of the Main Manuscript) were found to be of comparable energy and were thus considered in the subsequent RISM calculations performed for infinite dilution at ambient temperature.

We used the 1D-RISM Ornstein-Zernike integral equation[19] coupled with the 1D-Kovalenko-Hirata closure[20] to calculate the solute-solvent radial distribution functions (RDFs), $g_{ij}(r)$, and associated potentials of mean force (PMFs) between sites (atoms) i and j. Spatial distribution functions for solvent and counterion around ACh^+ and CCh^+ and the associated spatial PMFs were obtained with the 3D-RISM integral equation[21] coupled with the 3D Kovalenko-Hirata closure[22].

The atom coordinates, partial charges and the van der Waals interaction parameters of ACh^+ and CCh^+ in both conformations used as RISM input are summarized in Tables S1-S4. The van der Waals interaction parameters of all cation sites and of Cl^- were taken from the General Amber Force Field (GAFF).[23] For water a modified SPC/E model was used.[24] Site charges were calculated from the QM output with the ESP method.[25] Hydration structures were calculated with the rism1d and rism3d.snglpnt codes of the *AmberTools 16* package.[26] using the MDIIS (Modified Direct Inversion in the Iterative Subspace) iterative scheme.[27] The 1D-RISM equations were solved on an one-dimensional grid of 16384 points with a spacing of $2.5 \cdot 10^{-3}$ nm with 10 MDIIS vectors. For 3D-RISM a three-dimensional grid of $270 \times 270 \times 256$ points was chosen for AChCl(aq). For CChCl(aq) $270 \times 270 \times 280$ grid points with 4 MDIIS vectors was used. In both case the grid spacing was 0.025 nm and a residual tolerance of 10^{-6} was chosen. The used grid parameters are large enough to accommodate the ions together with sufficient solvation space around them so that the obtained results are without significant numerical errors.

Determination of activation energies

The relaxation time of ACh^+, τ_1, determined for aqueous AChCl solution molalities of $m = 0.2621\,\mathrm{mol\,kg^{-1}}$ and $0.3738\,\mathrm{mol\,kg^{-1}}$ scatter considerably (Table S11, Fig. S10). Accordingly, the data for both concentrations was pooled and its temperature dependence fitted by a simple Arrhenius equation

$$\tau_1 = \tau_0 \times \exp[E_\mathrm{a}/(RT)] \tag{S7}$$

with pre-exponential factor $\tau_0 = 4.0 \cdot 10^{-14}\,\mathrm{s}$ and activation energy $E_\mathrm{a} = (19 \pm 3)\,\mathrm{kJ\,mol^{-1}}$. The equivalent (standard) Eyring equation

$$\tau_1 = \frac{k_\mathrm{B}T}{h} \times \exp\left[(\Delta H^{\neq} - T\Delta S^{\neq})/(RT)\right] \tag{S8}$$

yielded the activation enthalpy of $\Delta H^{\neq} = (17 \pm 3)\,\mathrm{kJ\,mol^{-1}}$ and the corresponding activation entropy of $\Delta S^{\neq} = (3 \pm 10)\,\mathrm{J\,K^{-1}mol^{-1}}$.

The bulk-water relaxation times, τ_3, for both concentrations of Table S11 agreed within experimental uncertainty and thus were also pooled. The data exhibited a very smooth temperature dependence with clear curvature of the Arrhenius plot, Fig. S10. Accordingly, $\tau_3(T)$ was fitted with an extended Eyring equation[9]

$$\tau_3 = \frac{k_\mathrm{B}T}{h} \times \exp\left[[\Delta H^{\neq}_{298} + \Delta c_p^{\neq} \times (T - T_\mathrm{ref}) - T \times (\Delta S^{\neq}_{298} + \Delta c_p^{\neq} \times \ln \frac{T}{T_\mathrm{ref}})]/(RT)\right] \tag{S9}$$

where $T_\mathrm{ref} = 298.15\,\mathrm{K}$ to yield values for activation enthalpy, $\Delta H^{\neq}_{298} = (14.9 \pm 0.3)\,\mathrm{kJ\,mol^{-1}}$, entropy, $\Delta S^{\neq}_{298} = (16.8 \pm 0.8)\,\mathrm{J\,K^{-1}mol^{-1}}$, and heat capacity, $\Delta c_p^{\neq} = -(93 \pm 22)\,\mathrm{J\,K^{-1}mol^{-1}}$, comparable to data for pure water ($\Delta H^{\neq}_{298} = (16.09 \pm 0.07)\,\mathrm{kJ\,mol^{-1}}$, $\Delta S^{\neq}_{298} = (21.2 \pm 0.2)\,\mathrm{J\,K^{-1}mol^{-1}}$, $\Delta c_p^{\neq} = -(94 \pm 6)\,\mathrm{J\,K^{-1}mol^{-1}}$).[9]

The Eyring activation enthalpy of cation transport at the limit of infinite dilution, $\Delta H^{\ddagger}(\lambda_+^\infty)$ was determined with the Brummer-Hill equation[28]

$$\ln \lambda_+^\infty + \frac{2}{3} \ln \rho(0) = -\frac{\Delta H^{\ddagger}(\lambda_+^\infty)}{RT} + B \tag{S10}$$

where B is an empirical parameter and $\rho(0)$ the solvent density.[2] As expected from the very similar λ_+^∞ values (Table S7), $\mathrm{ACh^+}$ ($\Delta H^{\ddagger}(\lambda_+^\infty) = (14.7 \pm 0.3)\,\mathrm{kJ\,mol^{-1}}$) and $\mathrm{CCh^+}$ ($\Delta H^{\ddagger}(\lambda_+^\infty) = (14.8 \pm 0.3)\,\mathrm{kJ\,mol^{-1}}$) have practically identical enthalpies of transport.

Friction coefficients of dipole rotation

For rotational diffusion as the mechanism behind a Debye-type dielectric relaxation process, j, in the overall relaxation, eqn (S6), the rotational correlation time, τ'_j, of the rotating dipole should follow the generalized Stokes-Einstein-Debye (SED) equation

$$\tau'_j = \frac{V_\mathrm{eff}\eta}{k_\mathrm{B}T} + \tau_j^0 \tag{S11}$$

where V_eff is the effective volume of the dipole and τ_j^0 the empirically found intercept.[29] The effective volume, $V_\mathrm{eff} = V_\mathrm{m} f_\perp C$, is determined by the molecular volume of the dipole, V_m, a shape factor, $f_\perp$, relating V_m to the volume swept out by the dipole during rotation, and a hydrodynamic coupling parameter, C, connecting local friction to macroscopic viscosity, η. For the latter theoretical limits are $C = 1$ for dipole rotation with *stick* boundary conditions and $C = 1 - f_\perp^{-2/3}$ for *slip* rotation.

For a Debye-type mode the required single-molecule rotational correlation time, τ'_j, is obtained from the associated (collective) dielectric relaxation time, τ_j, as

$$\tau'_j = \frac{2\varepsilon_j + \varepsilon_{\infty,j}}{3\varepsilon_j} \times \tau_j \tag{S12}$$

where $\varepsilon_j = \varepsilon_\infty + \sum_j^n S_i$ $(j \leq i \leq n)$ and $\varepsilon_{\infty,j} = \varepsilon_\infty + \sum_{j+1}^n S_i$ define the low- and high-frequency limits of mode j in the overall relaxation defined by eqn (S6).[30]

For the reorientation of the solute cations ACh^+ and CCh^+, associated with mode 1 of the present spectra, rotational diffusion was expected. Indeed, plots of the their respective rotational correlation times, τ_1', obtained with eqn (S12) from the data of Tables S10 and S11, against viscosity (not shown) were reasonably linear, albeit with a slight systematic curvature suggesting a weak concentration dependence of local friction.

Assuming validity of eqn (S11) and inserting the values of $V_\mathrm{m} = 0.222\,\mathrm{nm}^3$ and $f_\perp = 1.17$ for ACh^+ and $V_\mathrm{m} = 0.215\,\mathrm{nm}^3$ and $f_\perp = 1.24$ for CCh^+ from the Gaussian output, the hydrodynamic coupling parameters, C, of Fig. S11 were obtained. For CCh^+ values of $C \approx 0.2$ were found, which are very close to the *slip* limit (0.134). Those of ACh^+ are somewhat larger ($C \approx 0.4$). For both cations C appears to decrease slightly with increasing solute concentration.

Standard-state association constant from DRS

Ion-pair concentrations, c_IP, of CChCl(aq) were calculated with eqn (**??**) from the amplitudes, S_0, of the lowest-frequency mode. Linear contact ion pairs (CIPs, insert of Fig. S14) with an effective dipole moment of $\mu_\mathrm{eff} = 19.8\,\mathrm{D}$ (Gaussian09 at B3LIP/6-31G(d,p) level, PCM solvation model) were assumed.

The thus accessible association numbers, $K_\mathrm{A}(c) = c_\mathrm{IP}/(c - c_\mathrm{IP})^2$ (in M^{-1}), were fitted as a function of the stoichiometric ionic strength, $I(= c)$, with an extended Guggenheim-type equation[31]

$$\log K_\mathrm{A} = \log K_\mathrm{A}^\circ - \frac{2A_\mathrm{DH}\,|z_+ z_-|\,\sqrt{I}}{1+\sqrt{I}} + B \cdot I + C \cdot I^{3/2} \tag{S13}$$

to yield the standard-state (infinite dilution) association constant, $K_\mathrm{A}^\circ = (16 \pm 5)\,\mathrm{M}^{-1}$ (Fig. S14). In eqn (S13) $z_+ = |z_-| = 1$ are the ion charge numbers, $A_\mathrm{DH} = 0.5115\,(\mathrm{L\,mol^{-1}})^{1/2}$ is the Debye-Hückel constant for activity coefficients in water at 298.15 K, and $B = -3.07\,\mathrm{M}^{-1}$ and $C = 1.36\,\mathrm{M}^{-3/2}$ are adjusted parameters.

Supplementary Tables

Table S1: Coordinates of the atoms, x, y and z, van der Waals parameters, σ_{vdW} and $\varepsilon_{\mathrm{vdW}}$, and partial charges, q, of the atoms of ACh$^+$ in its TG conformation in water at 298.15 K. For site designations see Fig. 1 of the Main Manuscript.

site	x / nm	y / nm	z / nm	σ / nm	ε / kcal mol^{-1}	q
Cc	0.308	-0.020	0.153	0.340	0.086	0.848
Oc	0.344	-0.062	0.045	0.296	0.210	-0.612
Cm1	0.381	-0.039	0.284	0.340	0.109	-0.611
Hm1	0.323	-0.105	0.348	0.265	0.016	0.192
Hm1	0.479	-0.083	0.265	0.265	0.016	0.171
Hm1	0.392	0.057	0.336	0.265	0.016	0.193
O	0.194	0.050	0.171	0.300	0.170	-0.446
Cb1	0.113	0.072	0.053	0.340	0.109	0.260
Hb1	0.170	0.129	-0.021	0.247	0.016	0.044
Hb1	0.087	-0.024	0.007	0.247	0.016	0.082
Cb2	-0.018	0.139	0.092	0.340	0.109	-0.292
Hb2	-0.081	0.140	0.002	0.196	0.016	0.174
Hb2	-0.069	0.081	0.170	0.196	0.016	0.198
N	0.011	0.283	0.142	0.325	0.170	0.253
Cm	0.043	0.291	0.283	0.340	0.109	-0.386
Cm	0.072	0.370	0.051	0.340	0.109	-0.468
Cm	-0.153	0.337	0.143	0.340	0.109	-0.447
Hm	-0.152	0.438	0.185	0.196	0.016	0.213
Hm	-0.191	0.338	0.041	0.196	0.016	0.210
Hm	-0.214	0.271	0.206	0.196	0.016	0.200
Hm	0.04	0.396	0.315	0.196	0.016	0.197
Hm	-0.019	0.230	0.348	0.196	0.016	0.194
Hm	0.146	0.254	0.283	0.196	0.016	0.175
Hm	0.061	0.474	0.083	0.196	0.016	0.207
Hm	0.177	0.341	0.059	0.196	0.016	0.229
Hm	0.037	0.358	-0.052	0.196	0.016	0.220

Table S2: Coordinates of the atoms, x, y and z, van der Waals parameters, σ_{vdW} and $\varepsilon_{\mathrm{vdW}}$, and partial charges, q, of the atoms of ACh^+ in its TT conformation in water at 298.15 K. For site designations see Fig. 1 of the Main Manuscript.

site	x / nm	y / nm	z / nm	σ / nm	ε / kcal mol^{-1}	q
Cc	0.305	-0.023	0.171	0.340	0.086	0.861
Oc	0.367	-0.051	0.070	0.296	0.210	-0.622
Cm1	0.346	-0.054	0.313	0.340	0.109	-0.588
Hm1	0.281	-0.132	0.353	0.265	0.016	0.189
Hm1	0.449	-0.089	0.314	0.265	0.016	0.167
Hm1	0.335	0.035	0.376	0.265	0.016	0.184
O	0.185	0.040	0.168	0.300	0.170	-0.506
Cb1	0.133	0.074	0.038	0.340	0.109	0.388
Hb1	0.205	0.136	-0.015	0.247	0.016	0.034
Hb1	0.117	-0.018	-0.019	0.247	0.016	0.033
Cb2	0.003	0.147	0.070	0.340	0.109	-0.278
Hb2	-0.063	0.081	0.128	0.196	0.016	0.184
Hb2	0.024	0.236	0.130	0.196	0.016	0.183
N	-0.077	0.193	-0.051	0.325	0.170	0.161
Cm	0.003	0.291	-0.135	0.340	0.109	-0.341
Cm	-0.120	0.076	-0.136	0.340	0.109	-0.349
Cm	-0.201	0.264	0.001	0.340	0.109	-0.473
Hm	-0.062	0.330	-0.213	0.196	0.016	0.190
Hm	0.038	0.372	-0.070	0.196	0.016	0.193
Hm	0.087	0.239	-0.180	0.196	0.016	0.170
Hm	-0.259	0.298	-0.085	0.196	0.016	0.224
Hm	-0.259	0.194	0.061	0.196	0.016	0.217
Hm	-0.169	0.349	0.062	0.196	0.016	0.217
Hm	-0.186	0.114	-0.215	0.196	0.016	0.192
Hm	-0.033	0.029	-0.181	0.196	0.016	0.175
Hm	-0.174	0.005	-0.073	0.196	0.016	0.195

Table S3: Coordinates of the atoms, x, y and z, van der Waals parameters, σ_{vdW} and $\varepsilon_{\mathrm{vdW}}$, and partial charges, q, of the atoms of CCh^+ in its TG conformation in water at 298.15 K. For site designations see Fig. 1 of the Main Manuscript.

site	x / nm	y / nm	z / nm	σ / nm	ε / kcal mol^{-1}	q
Cm	-0.145	-0.169	-0.254	0.340	0.109	-0.452
Hm	-0.179	-0.228	-0.340	0.196	0.016	0.207
Hm	-0.130	-0.065	-0.282	0.196	0.016	0.207
Hm	-0.053	-0.212	-0.214	0.196	0.016	0.227
N	-0.253	-0.176	-0.147	0.325	0.170	0.213
Cm	-0.383	-0.130	-0.208	0.340	0.109	-0.414
Hm	-0.460	-0.129	-0.130	0.196	0.016	0.192
Hm	-0.411	-0.199	-0.288	0.196	0.016	0.209
Hm	-0.369	-0.029	-0.248	0.196	0.016	0.202
Cm	-0.269	-0.320	-0.101	0.340	0.109	-0.455
Hm	-0.351	-0.324	-0.030	0.196	0.016	0.211
Hm	-0.176	-0.353	-0.055	0.196	0.016	0.207
Hm	-0.291	-0.381	-0.189	0.196	0.016	0.216
Cb2	-0.223	-0.085	-0.028	0.340	0.109	-0.134
Hb2	-0.244	0.017	-0.060	0.196	0.016	0.154
Hb2	-0.295	-0.113	0.049	0.196	0.016	0.153
Cb1	-0.082	-0.092	0.030	0.340	0.109	0.182
Hb1	-0.087	-0.067	0.137	0.247	0.016	0.091
Hb1	-0.034	-0.190	0.021	0.247	0.016	0.069
O	-0.002	0.010	-0.037	0.300	0.170	-0.485
Cc	0.128	0.024	0.002	0.340	0.086	1.068
Oc	0.185	-0.056	0.077	0.296	0.210	-0.767
Na	0.185	0.132	-0.054	0.325	0.170	-1.096
Ha	0.280	0.156	-0.027	0.107	0.016	0.495
Ha	0.130	0.200	-0.105	0.107	0.016	0.497

Table S4: Coordinates of the atoms, x, y and z, van der Waals parameters, σ_{vdW} and $\varepsilon_{\mathrm{vdW}}$, and partial charges, q, of the atoms of CCh$^+$ in its TT conformation in water at 298.15 K. For site designations see Fig. 1 of the Main Manuscript.

site	x / nm	y / nm	z / nm	σ / nm	ε / kcal mol^{-1}	q
Cm	-0.225	-0.313	-0.123	0.340	0.109	-0.330
Hm	-0.247	-0.371	-0.213	0.196	0.016	0.183
Hm	-0.123	-0.330	-0.091	0.196	0.016	0.167
Hm	-0.295	-0.339	-0.043	0.196	0.016	0.189
N	-0.244	-0.167	-0.157	0.325	0.170	0.174
Cm	-0.143	-0.126	-0.262	0.340	0.109	-0.324
Hm	-0.042	-0.149	-0.227	0.196	0.016	0.165
Hm	-0.154	-0.019	-0.282	0.196	0.016	0.188
Hm	-0.164	-0.184	-0.353	0.196	0.016	0.182
Cm	-0.383	-0.147	-0.213	0.340	0.109	-0.457
Hm	-0.393	-0.209	-0.302	0.196	0.016	0.218
Hm	-0.396	-0.041	-0.239	0.196	0.016	0.210
Hm	-0.456	-0.177	-0.137	0.196	0.016	0.210
Cb2	-0.233	-0.079	-0.033	0.340	0.109	-0.234
Hb2	-0.253	0.024	-0.065	0.196	0.016	0.166
Hb2	-0.312	-0.111	0.035	0.196	0.016	0.167
Cb1	-0.098	-0.083	0.040	0.340	0.109	0.426
Hb1	-0.073	-0.183	0.078	0.247	0.016	0.024
Hb1	-0.015	-0.047	-0.021	0.247	0.016	0.025
O	-0.118	0.007	0.152	0.300	0.170	-0.575
Cc	-0.013	0.026	0.237	0.340	0.086	1.120
Oc	0.096	-0.030	0.223	0.296	0.210	-0.784
Na	-0.045	0.112	0.336	0.325	0.170	-1.118
Ha	-0.137	0.154	0.343	0.107	0.016	0.507
Ha	0.025	0.134	0.407	0.107	0.016	0.502

Table S5: Molar conductivities, Λ, of aqueous AChCl solutions (density gradient $b = 0.0253\,\mathrm{kg^2L^{-1}mol^{-1}}$; molar mass $M = 181.66\,\mathrm{g\,mol^{-1}}$) as a function of solute molality, m, and temperature, T.

T / K	278.15	283.15	288.15	293.15	298.15	303.15	308.15	313.15
$m \cdot 10^3$ / mol kg^{-1}	Λ / S cm^{2}mol^{-1}							
0.44586	67.949	77.843	88.169	98.915	109.944	121.259	132.786	144.539
0.70122	67.455	77.292	87.586	98.308	109.321	120.620	131.990	143.425
1.06701	67.083	76.871	87.119	97.811	108.837	120.199	131.598	143.046
1.38843	66.823	76.582	86.801	97.471	108.487	119.845	131.490	143.210
1.9129	66.629	76.361	86.543	97.162	108.124	119.410	130.844	142.200
2.57467	66.325	76.005	86.136	96.715	107.615	118.864	130.264	141.510
3.44449	65.904	75.525	85.590	96.082	106.916	118.108	129.575	140.985
4.41039	65.466	75.029	85.025	95.448	106.209	117.328	128.703	139.891
5.51221	65.076	74.577	84.521	94.874	105.580	116.631	127.858	139.101
6.62949	64.681	74.125	84.006	94.300	104.941	115.930	127.211	138.565

Table S6: Molar conductivities, Λ, of aqueous CChCl solutions (density gradient $b = 0.0366\,\mathrm{kg^2L^{-1}mol^{-1}}$; molar mass $M = 182.65\,\mathrm{g\,mol^{-1}}$) as a function of solute molality, m, and temperature, T.

T / K	278.15	283.15	288.15	293.15	298.15	303.15	308.15	313.15
$m \cdot 10^3$ / $\mathrm{mol\,kg^{-1}}$	Λ / $\mathrm{S\,cm^2mol^{-1}}$							
0.19942	68.081	77.974	88.288	99.027	110.055	121.389	133.079	145.327
0.40808	67.521	77.308	87.585	98.299	109.303	120.672	132.396	144.485
0.60587	67.169	76.950	87.172	98.017	108.988	120.379	132.070	143.967
0.82557	67.143	76.923	87.133	97.766	108.706	120.041	131.736	143.691
1.13723	66.703	76.422	86.584	97.186	108.120	119.403	130.988	142.740
1.52406	66.385	76.063	86.177	96.731	107.607	118.832	130.172	141.494
1.98391	66.035	75.655	85.714	96.208	107.045	118.243	129.723	141.369
2.48942	65.738	75.309	85.330	95.783	106.573	117.705	129.082	140.465
3.16622	65.347	74.875	84.823	95.205	105.927	117.014	128.391	140.007
3.97644	64.980	74.442	84.331	94.651	105.306	116.299	127.417	138.678
4.86465	64.640	74.047	83.896	94.163	104.778	115.746	126.951	138.358
5.81694	64.334	73.692	83.494	93.709	104.280	115.178	126.397	137.775

Table S7: Limiting ionic conductivities, λ_+^∞, self-diffusion coefficients, D_+^∞, and hydrodynamic radii, r_{h+}, of the cations ACh$^+$ and CCh$^+$ in aqueous solution at temperature, T.[a]

	λ_+^∞		D_+^∞		r_{h+}	
T / K	ACh$^+$	CCh$^+$	ACh$^+$	CCh$^+$	ACh$^+$	CCh$^+$
278.15	23.47	23.25	5.835	5.780	0.230	0.232
283.15	25.23	24.95	6.385	6.314	0.248	0.251
288.15	28.10	27.75	7.237	7.148	0.256	0.259
293.15	31.59	31.21	8.279	8.178	0.259	0.262
298.15	35.28	34.82	9.404	9.279	0.261	0.264
303.15	39.08	38.59	10.589	10.456	0.263	0.266
308.15	42.88	42.56	11.812	11.722	0.265	0.267
313.15	46.73	46.82	13.081	13.107	0.268	0.268

[a] Units: T in K; λ_+^∞ in $\mathrm{S\,cm^2mol^{-1}}$; D_+^∞ in $10^{-10}\,\mathrm{m^2s^{-1}}$; r_{h+} in nm.

Table S8: Molar concentrations, c, densities, ρ, dynamic viscosities, η, and electrical conductivities, κ, as a function of solute concentration, c, of the DRS samples of AChCl(aq) and CChCl(aq) at 298.15 K.[a]

AChcl(aq)				CChCl(aq)			
c	ρ	η	κ	c	ρ	η	κ
0.0750	0.99891	0.892	0.678	0.0743	0.99977	0.911	0.661
0.1501	1.00073	0.916	1.258	0.1567	1.00262	0.924	1.277
0.2005	1.00203	0.930	1.634	0.2004	1.00415	0.935	1.573
0.2510	1.00333	0.945	1.985	0.2459	1.00576	0.946	1.927
0.3013	1.00454	0.961	2.280	0.3193	1.00832	0.965	2.394
0.3521	1.00588	0.979	2.643	0.3524	1.00948	0.974	2.774
0.4027	1.00708	0.994	2.906	0.4037	1.01126	0.985	3.090
0.4538	1.0084	1.014	3.181	0.4985	1.01459	1.039	3.682
0.5334	1.01035	1.045	3.604	0.8338	1.02627	1.131	5.360

[a] Units: c in mol·L^{-1}; ρ in kg·L^{-1}; η in 10^{-3} Pa·s; κ in S·m^{-1}.

Table S9: Molar concentrations, c, densities, ρ, dynamical viscosities, η, and electrical conductivities, κ, as a function of temperature, T, of aqueous AChCl solutions with $m = 0.2621\,\mathrm{mol\,kg^{-1}}$ and $m = 0.3738\,\mathrm{mol\,kg^{-1}}$.[a]

	$m = 0.2621\,\mathrm{mol\,kg^{-1}}$				$m = 0.3738\,\mathrm{mol\,kg^{-1}}$			
T	c	ρ	η	κ	c	ρ	η	κ
278.15	0.2519	1.00703	1.619	1.209	0.3535	1.00989	1.681	1.599
288.15	0.2516	1.00571	1.213	1.581	0.3530	1.00839	1.257	2.098
298.15	0.2510	1.00333	0.945	1.985	0.3521	1.00588	0.979	2.643
308.15	0.2502	1.00007	0.765	2.420	0.3510	1.00253	0.792	3.218
318.15	0.2492	0.99608	0.629	2.870	0.3495	0.99846	0.653	3.815
328.15	0.2480	0.99143	0.532	3.330	0.3479	0.99376	0.552	4.427
338.15	0.2467	0.98622	0.454	3.80	0.3460	0.98851	0.48	5.049

[a] Units: T in K; c in mol·L^{-1}; ρ in kg·L^{-1}; η in 10^{-3} Pa·s; κ in S·m^{-1}.

Table S10: Static permittivity, ε, relaxation amplitudes, S_j ($j = 1,..,4$), relaxation times, τ_j, high-frequency permittivity, ε_∞, of AChCl(aq) at 298.15 K.[a,b]

c	ε	S_1	τ_1	S_2	τ_2	S_3	τ_3	S_4	τ_4	ε_∞
0.0750	77.5	0.74	118.7	0.76	20.5	69.8	8.56	2.71	0.278F	3.52F
0.1501	76.9	1.72	79.5	1.17	19.3	67.6	8.61	2.88	0.278F	3.52F
0.2005	76.4	2.23	73.0	1.73	22.7	65.9	8.62	2.94	0.278F	3.52F
0.2510	76.3	2.77	71.6	2.6F	19.7	64.5	8.59	2.95	0.278F	3.52F
0.3013	75.8	2.49	83.8	3.8F	22.0	63.1	8.53	2.88	0.278F	3.52F
0.3521	75.3	2.65	86.2	4.19	22.8	61.9	8.67	3.12	0.278F	3.52F
0.4027	74.6	2.91	80.5	4.32	22.1	60.7	8.76	3.18	0.360	3.52F
0.4538	73.6	3.08	76F	4.29	19.8	58.8	9.04	3.88	0.862	3.52F
0.5334	73.2	3.59	71.2	5.32	23.0	57.4	8.96	3.43	0.632	3.52F

[a]Units: c in mol L^{-1}; τ_j in ps. [b]Parameter values followed by "F" were fixed during fitting.

Table S11: Static permittivity, ε, relaxation amplitudes, S_j ($j = 0\ldots3$), relaxation times, τ_l, and high-frequency permittivity, ε_∞, of CChCl(aq) at 298.15 K.[a,b]

c	ε	S_0	τ_0	S_1	τ_1	S_2	τ_2	S_3	τ_3	ε_∞
0.0743	78.1	1.37	604	0.36	119	–	–	70.5	8.42	5.90
0.1567	77.6	1.24	531	1.14	123	2.18	19.8	67.3	8.29	5.67
0.2004	77.0	1.22	416	1.43	116	2.43	21.1	66.2	8.31	5.73
0.2459	76.5	1.22	400F	1.68	116	3.30	20.2	64.7	8.29	5.66
0.3193	76.0	1.69	314	2.08	71.3	3.63	18.7	62.8	8.35	5.80
0.3524	75.8	1.68	360	2.01	91.7	4.27	20.2	62.0	8.36	5.83
0.4037	75.7	1.91	350F	2.72	79.0	5.52	18.4	59.7	8.34	5.80
0.4985	75.4	2.47	400F	3.47	75.3	6.56	16.9	56.9	8.40	5.98
0.8338	72.2	2.00	464	4.44	101	12.1	19F	47.8	8.34	5.86

[a]Units: c in mol L^{-1}; τ_l in ps. [b]Parameter values followed by "F" were fixed during fitting.

Table S12: Static permittivity, ε, relaxation amplitudes, S_j ($j = 1 \ldots 4$), relaxation times, τ_j, high-frequency permittivity, ε_∞, of AChCl(aq) concentrations $m = 0.2621\,\mathrm{mol\,kg^{-1}}$ (0.2510 M at 298.15 K) and $0.3738\,\mathrm{mol\,kg^{-1}}$ (0.3521 M at 298.15 K) as a function of temperature, T.[a,b]

T	ε	S_1	τ_1	S_2	τ_2	S_3	α_3	τ_3	S_4	τ_4	ε_∞
$b = 0.2621\,\mathrm{mol\,kg^{-1}}$											
278.15	83.6	2.60	162	6.78	27.8	67.8	–	14.7	2.47	0.480	3.96F
288.15	79.6	2.08	125	5.07	25.2	65.9	–	11.0	2.85	0.831	3.68F
298.15	76.3	2.77	71.6	2.6F	19.7	64.5	–	8.59	2.95	0.278F	3.52F
308.15	72.7	1.28	115	–	–	67.1	0.035	6.90	1.13	0.212F	3.2F
318.15	69.3	1.16	110	–	–	64.1	0.031	5.58	1.33	0.17F	2.78F
328.15	66.3	2.82	43.0	–	–	57.5	–	4.70	3.22	0.189F	2.8F
338.15	64.3	3.02	43.7	–	–	55.0	–	4.00	3.70	0.128F	2.58F
$b = 0.3738\,\mathrm{mol\,kg^{-1}}$											
278.15	83.0	2.79	241	9.82	33F	63.5	–	14.9	2.92	0.509F	3.96F
288.15	78.7	2.39	129	8.03	26.5	62.2	–	10.8	2.41	0.288	3.68F
298.15	75.3	2.65	86.2	4.19	22.8	61.9	–	8.67	3.12	0.278F	3.52F
308.15	71.8	2.99	62.7	–	–	63.2	0.017	7.11	2.42	0.212F	3.2F
318.15	68.6	2.45	71.2	–	–	60.8	0.020	5.79	2.63	0.17F	2.78F
328.15	65.5	3.52	35.1	–	–	55.7	–	4.85	3.39	0.189F	2.84F
338.15	63.1	3.38	39.5	–	–	53.5	–	4.13	3.62	0.128F	2.58F

[a] Units: T in K; τ_j in ps. [b] Parameter values followed by “F” were fixed during fitting.

Table S13: Structural parameters of ACh^+ and CCh^+ hydration for their TG and TT conformers in aqueous solution at 25 °C and infinite dilution: Maximum values of radial distribution functions, $g_{ij}(r_{ij,\mathrm{M1}})$, at distance, $r_{ij,\mathrm{M1}}$, and associated coordination numbers, n_{ij}. For the site labelling see Fig. 1 of the Main Manuscript.

	ACh^+		CCh^+	
	TG	TT	TG	TT
	$-N^+(CH_3)_3$ moiety			
g_{NOw}	1.53	1.54	1.53	1.54
$r_{\mathrm{NOw,M1}}$ / nm	0.426	0.428	0.428	0.430
n_{NOw}	19	22.9	20	24.2
g_{CmOw}	1.51	1.58	1.58	1.59
$r_{\mathrm{CmOw,M1}}$ / nm	0.312	0.310	0.312	0.312
n_{CmOw}	5.8	5.9	6.1	6.2
g_{HmOw}	0.77-1.06	1.00-1.06	0.95-1.09	1.00-1.08
$r_{\mathrm{HmOw,M1}}$ / nm	0.230-0.240	0.233-0.235	0.230-0.235	0.233-0.235
	$-CH_2-$ groups (‘b1’ and ‘b2’ in Fig. 1)			
g_{Cb1Ow}	1.25	1.22	1.22	1.18
$r_{\mathrm{Cb1Ow,M1}}$ / nm	0.340	0.340	0.340	0.340
n_{Cb1Ow}	10.3	10.4	9.9	10.1
g_{Hb1Ow}	1.01	1.06	1.14	1.11
$r_{\mathrm{Hb1Ow,M1}}$ / nm	0.250	0.250	0.250	0.250
g_{Cb2Ow}	1.16	1.12	1.09	1.09
$r_{\mathrm{Cb2Ow,M1}}$ / nm	0.315	0.315	0.315	0.315
n_{Cb2Ow}	4.1	3.9	3.8	3.8
g_{Hb2Ow}	1.08	1.02	1.04	1.00
$r_{\mathrm{Hb2Ow,M1}}$ / nm	0.233	0.233	0.233	0.233
	C=O group (‘c’ in Fig. 1)			
g_{OcOw}	1.76	1.75	1.81	1.79
$r_{\mathrm{OcOw,M1}}$ / nm	0.297	0.297	0.295	0.295
n_{OcOw}	6.4	6.3	6.2	6.2
g_{OcHw}	1.53	1.54	2.04	2.02
$r_{\mathrm{OcHw,M1}}$ / nm	0.173	0.173	0.170	0.170
n_{OcHw}	1.7	1.7	2.2	2.1

Table S13: Continued structural parameters of ACh^+ and CCh^+ hydration for their TG and TT conformers in aqueous solution at 25 °C and infinite dilution: Maximum values of radial distribution functions, $g_{ij}(r_{ij,\mathrm{M1}})$, at distance, $r_{ij,\mathrm{M1}}$, and associated coordination numbers, n_{ij}. For the site labelling see Fig. 1 of the Main Manuscript.

	ACh^+		CCh^+	
	TG	TT	TG	TT
		O atom		
g_{OOw}	0.90	1.14	0.98	1.16
$r_{\mathrm{OOw,M1}}$ / nm	0.305	0.305	0.305	0.305
n_{OOw}	3.1	4.2	3.2	4.1
g_{OHw}	0.29	0.44	0.30	0.44
$r_{\mathrm{OHw,M1}}$ / nm	0.182	0.180	0.185	0.180
	–CH_3 group ('m1' in Fig. 1)		–NH_2 group ('a' in Fig. 1)	
g_{Cm1Ow}, g_{NaOw}*	1.53	1.49	1.97	1.97
$r_{\mathrm{Cm1Ow,M1}}$, $r_{\mathrm{NaOw,M1}}$ / nm	0.338	0.338	0.297	0.297
n_{Cm1Ow}, n_{NaOw}	12.9	12.2	6.6	6.2
g_{Hm1Ow}, g_{NaHw}	1.20	1.20	0.26	0.26
$r_{\mathrm{HOw,M1}}$, $r_{\mathrm{NaHw,M1}}$ / nm	0.267	0.267	0.188	0.188
g_{HaOw}			1.41	1.42
$r_{\mathrm{HaOw,M1}}$ / nm			0.173	0.173
n_{HaOw}			0.7	0.7
		total coordination number		
n	30	32	29	30

*Note that Na stands for nitrogen atom (N) with label 'a', see Fig. 1b

Supplementary Figures

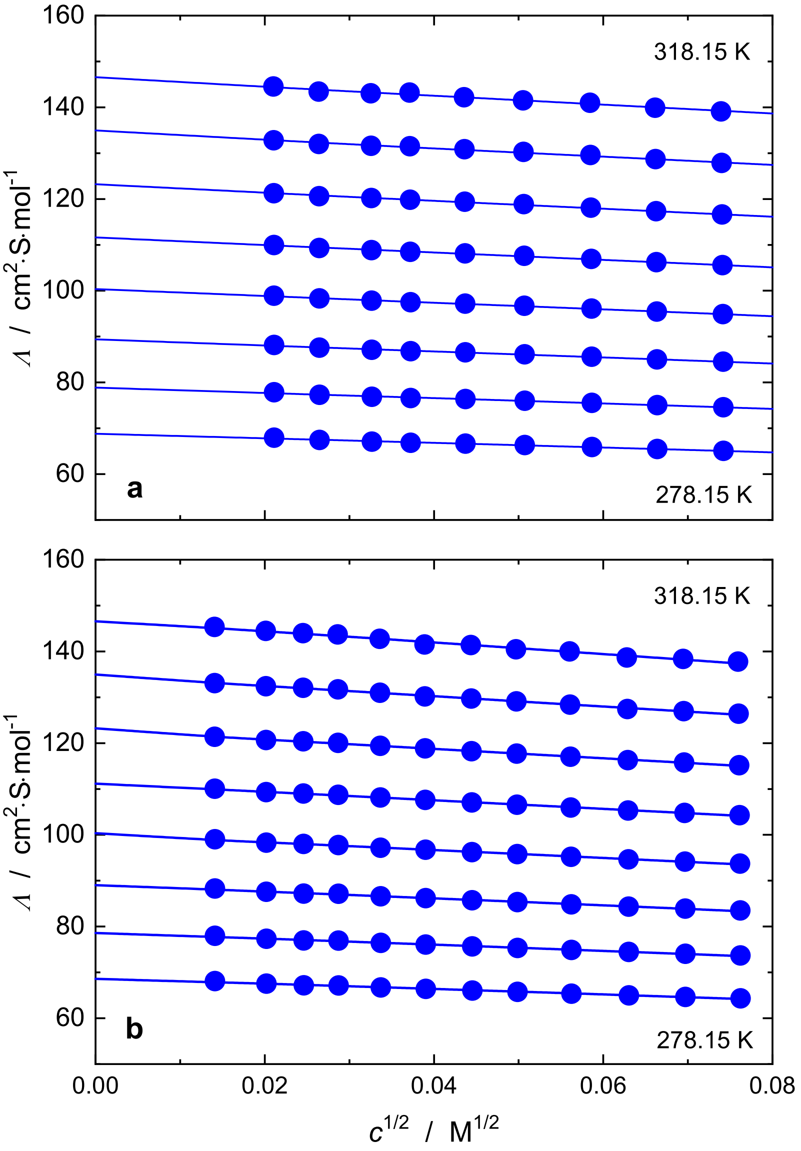

Figure S1: Molar conductivities, Λ (symbols), of aqueous AChCl (a) and CChCl (b) solutions as a function of solute concentration, c, and temperature, T, between 278.15 K and 313.15 K in steps of 5 K. Lines represent fits with the lcCM model.

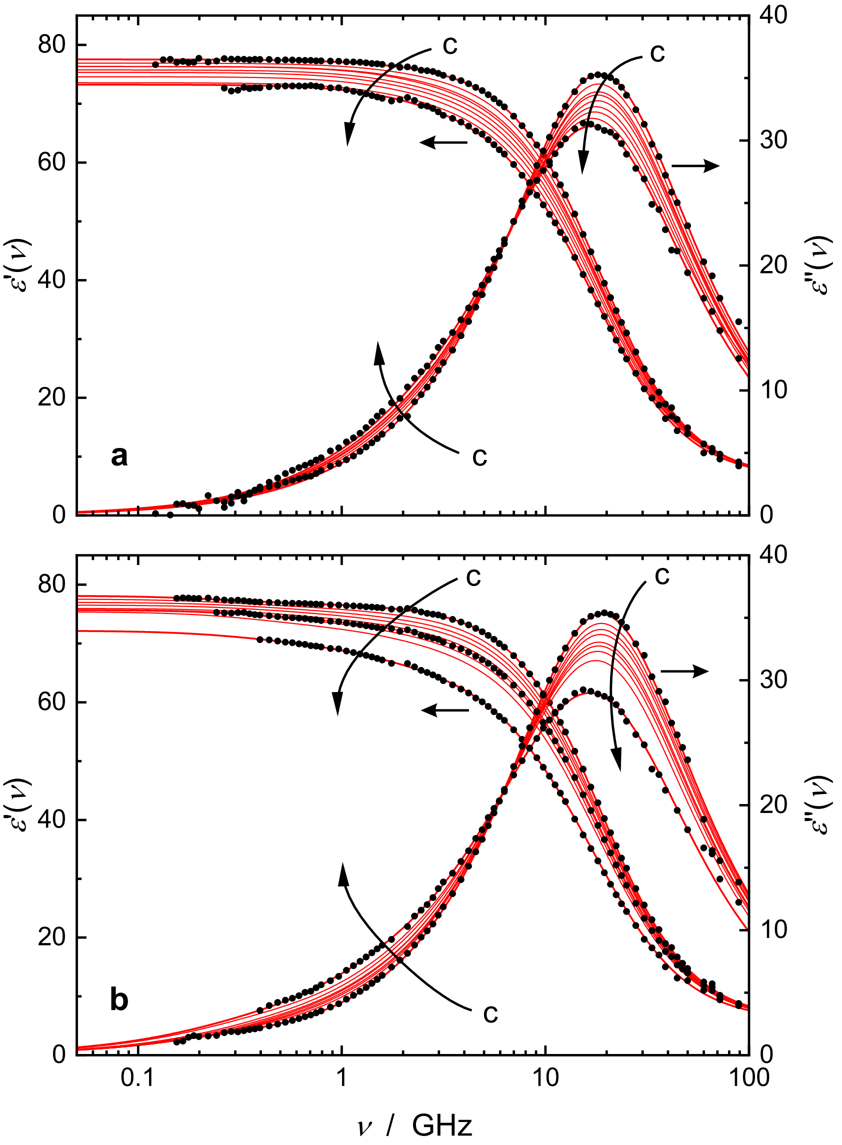

Figure S2: Relative permittivity, $\varepsilon'(\nu)$, and dielectric loss, $\varepsilon''(\nu)$, spectra of aqueous (a) AChCl for $0.0750 \leq c\,/\,\mathrm{M} \leq 0.5334$ and (b) CChCl for $0.0743 \leq c\,/\,\mathrm{M} \leq 0.8338$ at 298.15 K. The symbols represent the experimental data (partly omitted for visual clarity) and the lines the fits of the 4D model. The arrows indicate the data trend with increasing c.

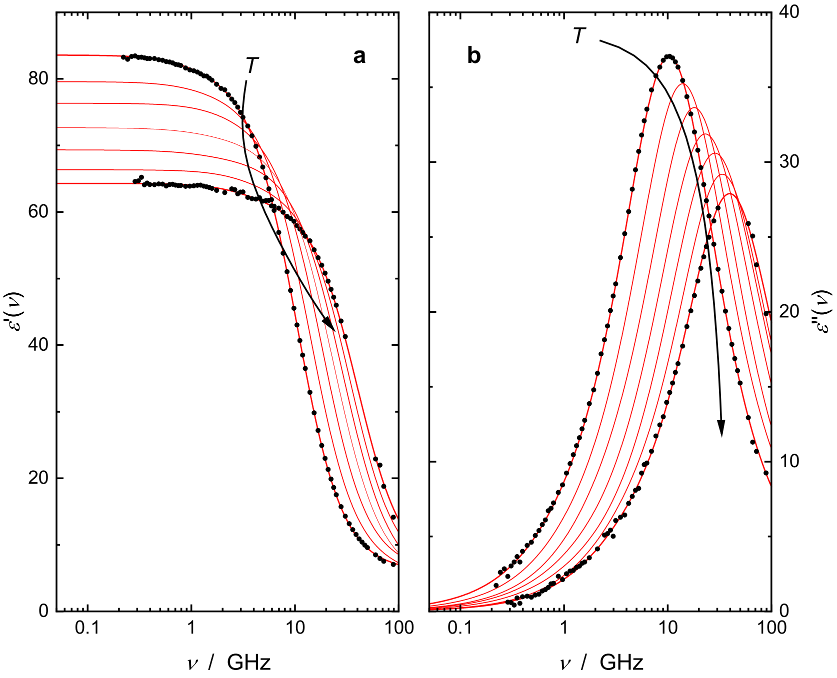

Figure S3: (a) Relative permittivity, $\varepsilon'(\nu)$, and (b) dielectric loss, $\varepsilon''(\nu)$, spectra of $0.2621\,\mathrm{mol\,kg^{-1}}$ aqueous AChCl from 278.15 K to 338.15 K in steps of 10 K (increasing in arrow direction). The symbols represent the experimental data (partly omitted for visual clarity) and the lines the fits of the D+D+CC+D model.

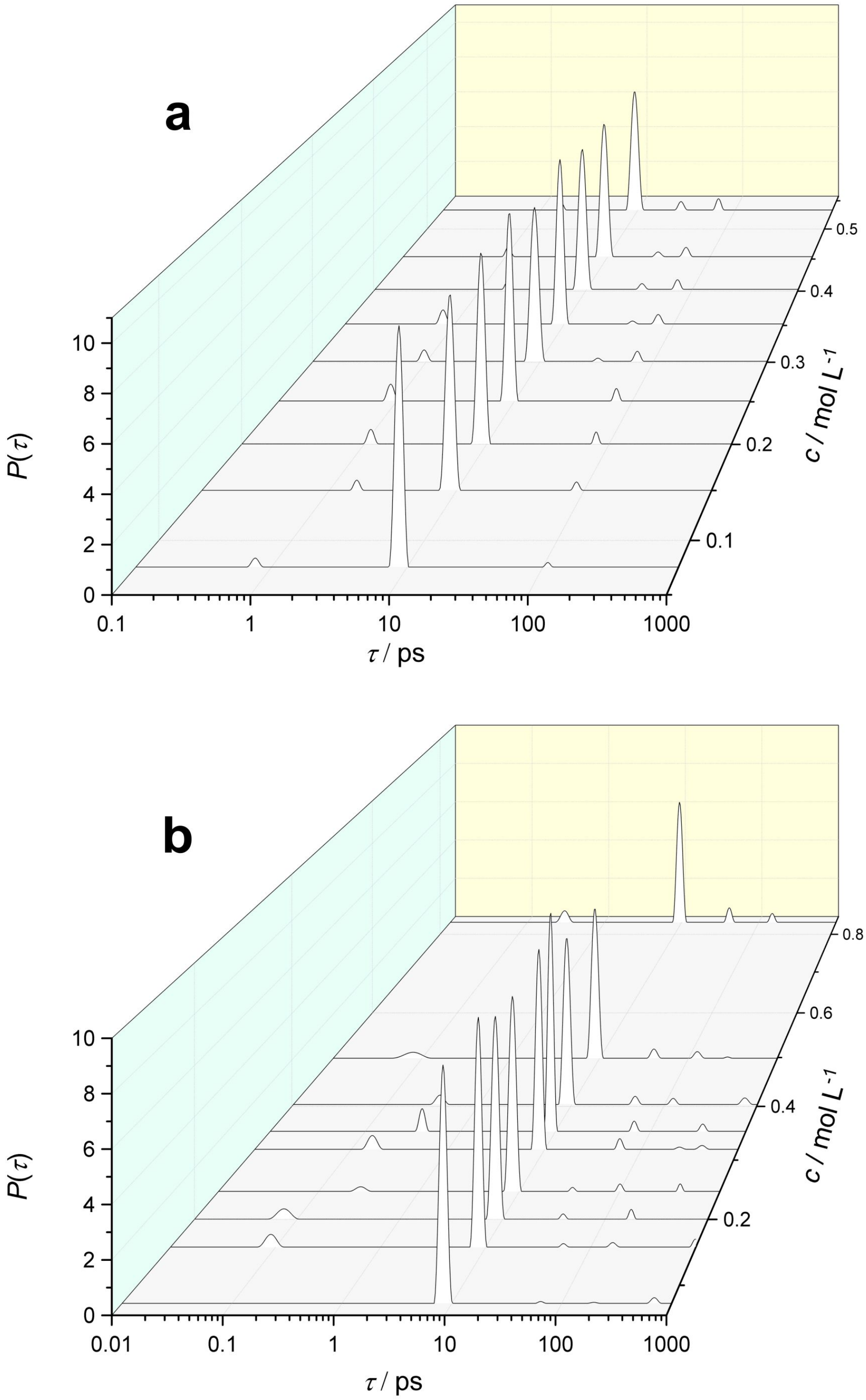

Figure S4: Relaxation time distribution functions, $P(\tau)$,[32] of the dielectric spectra of (a) AChCl(aq) and (b) CChCl(aq) at 298.15 K.

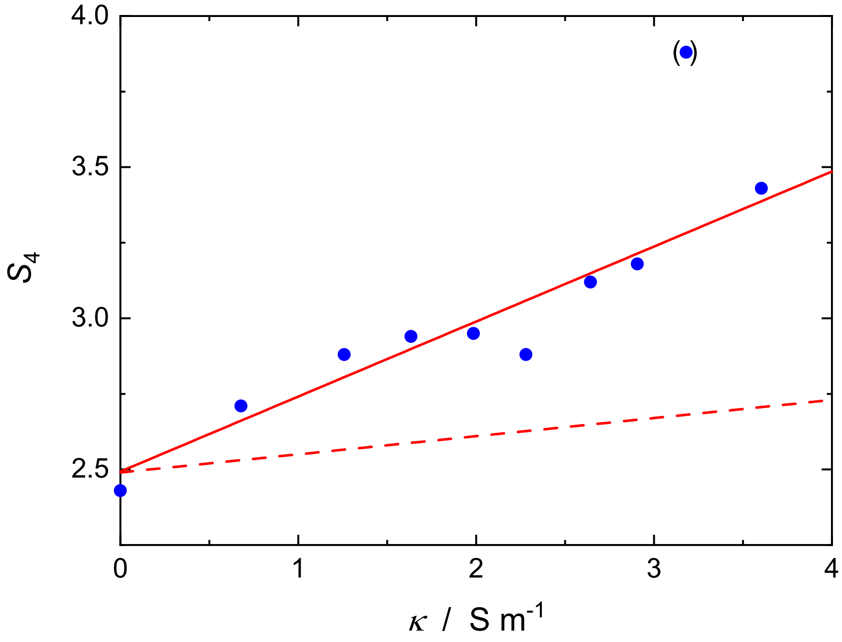

Figure S5: Amplitude, S_4 (●), of the fast water mode of AChCl(aq) as a function of the electrical conductivity, κ, of the solutions at 298.15 K. The solid line shows a straight-line fit to the data (bracketed point not included). The broken line shows the variation of S_4 with κ expected from the results of Balos et al.[33] for inorganic salts.

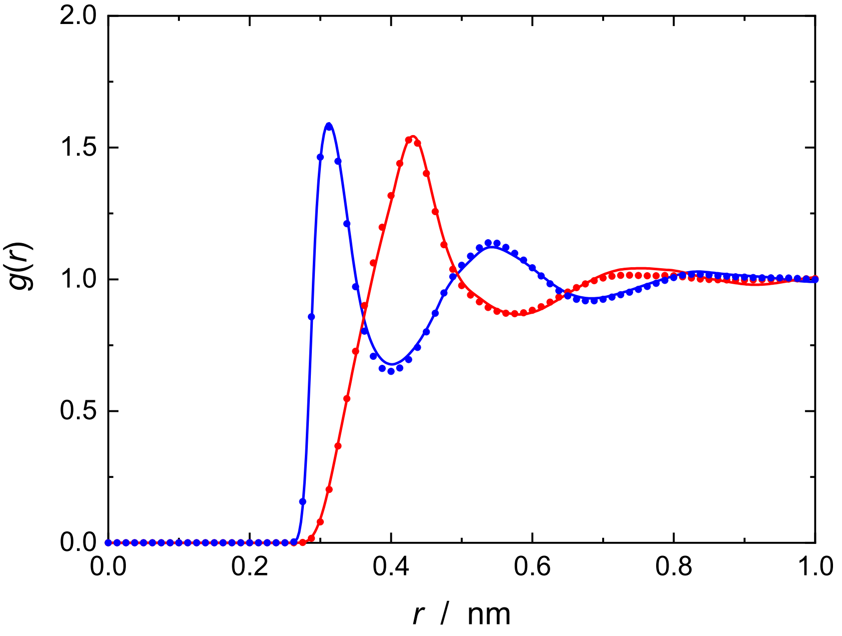

Figure S6: Radial distribution functions $g_{\mathrm{CmOw}}(r)$ (blue) and $g_{\mathrm{NOw}}(r)$ (red) for the trimethylammonium moiety of the TT conformations of CCh^+ (lines) and ACh^+ (symbols)[34] at infinite dilution in aqueous solution. For atom labelling see Fig. 1 of the Main Manuscript.

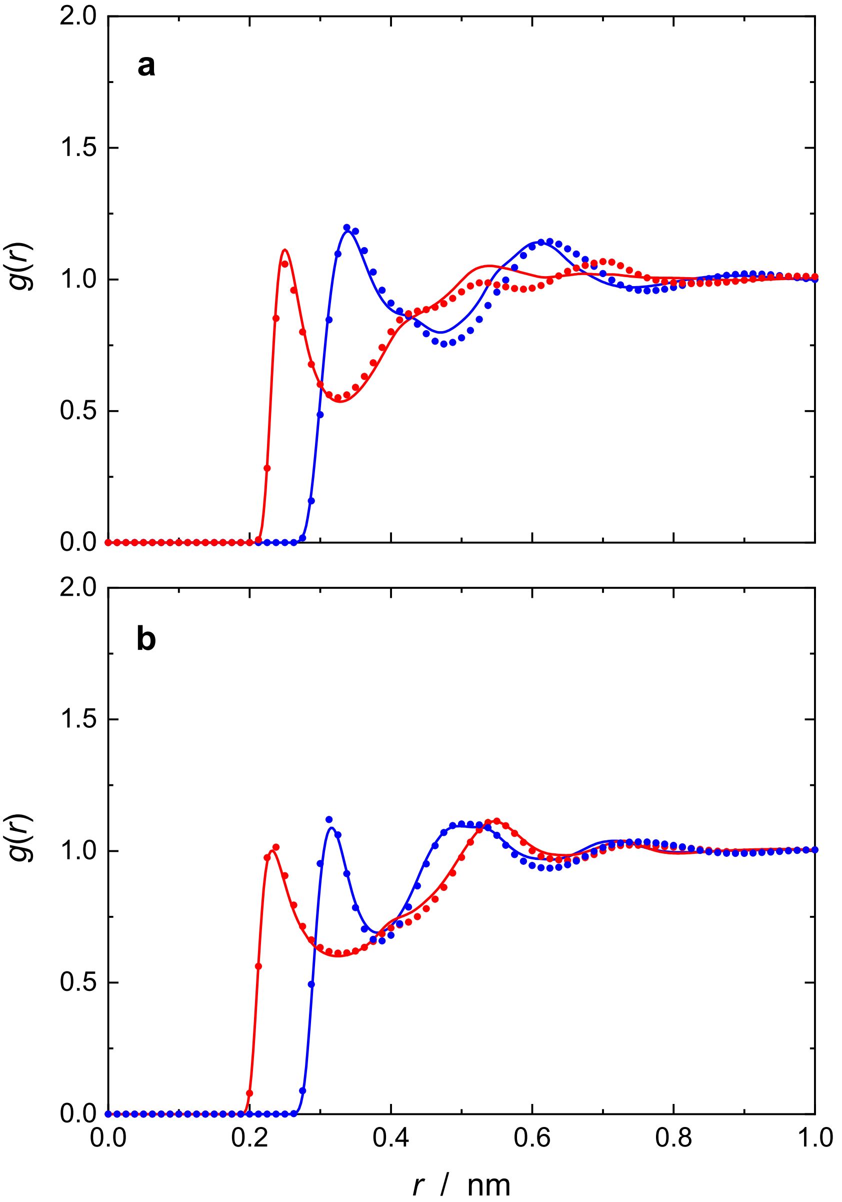

Figure S7: (a) Radial distribution functions $g_{\mathrm{Cb1Ow}}(r)$ (blue) and $g_{\mathrm{Hb1Ow}}(r)$ (red) for the TT conformations of CCh$^+$ (lines) and ACh$^+$ (symbols)[34] at infinite dilution in aqueous solution. (b) Corresponding RDFs $g_{\mathrm{Cb2Ow}}(r)$ (blue) and $g_{\mathrm{Hb2Ow}}(r)$ (red). For atom labelling see Fig. 1 of the Main Manuscript.

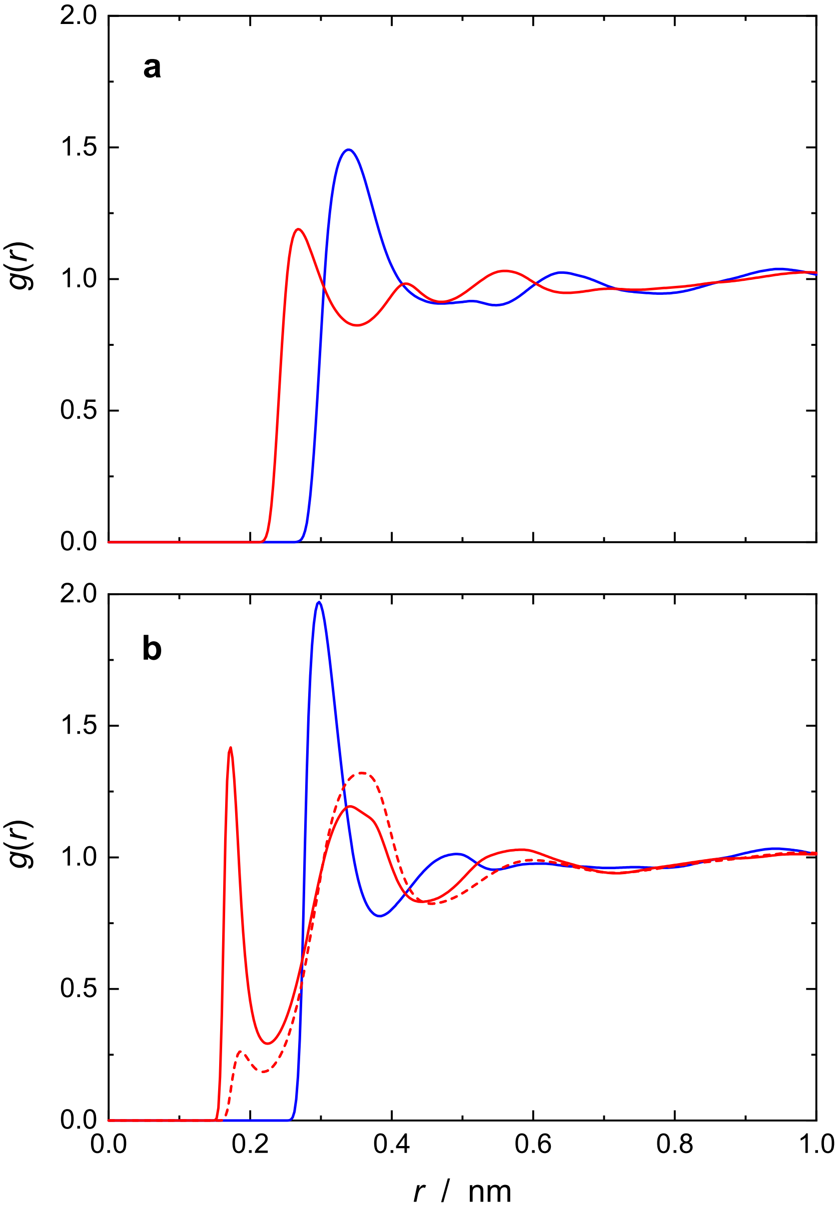

Figure S8: (a) Radial distribution functions $g_{\mathrm{Cm1Ow}}(r)$ (blue line) and $g_{\mathrm{Hm1Ow}}(r)$ (red line) for the *TT* conformation of ACh^+ at infinite dilution in aqueous solution.[34] (b) Radial distribution functions $g_{\mathrm{NaOw}}(r)$ (blue line), $g_{\mathrm{NaHw}}(r)$ (red broken line) and $g_{\mathrm{HaOw}}(r)$ (red solid line) for the TT conformation of CCh^+(aq). For atom labelling see Fig. 1 of the Main Manuscript.

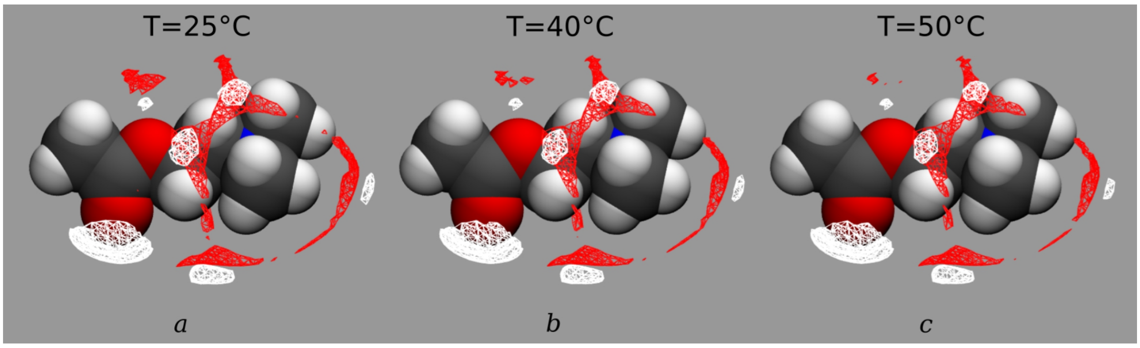

Figure S9: Spatial distribution functions of the oxygen (red) and hydrogen (white) atoms of water around *TT* ACh^+ at 25 °C (a), 40 °C (b) and 50 °C (c). The isodensity surfaces correspond to SDF values of $g_{\mathrm{catOw}}(\boldsymbol{r}) = 3.3$ and $g_{\mathrm{catHw}}(\boldsymbol{r}) = 2.0$.

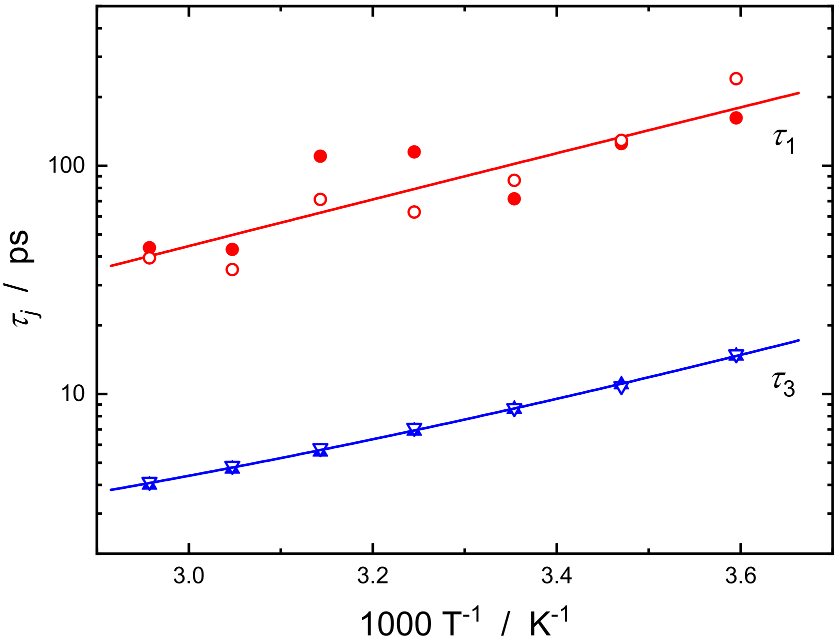

Figure S10: Arrhenius plots of the relaxation times of ACh$^+$, τ_1 (●, ○), and bulk water, τ_3 (▲, ▽), of aqueous solutions of 0.2621 mol kg^{-1} (closed symbols) and 0.3738 mol kg^{-1} (open symbols) AChCl as a function of temperature, T. The lines show an Arrhenius fit, eq S7, for τ_1 and a fit with the extended Eyring equation, eq S9, for τ_3 (all data pooled).

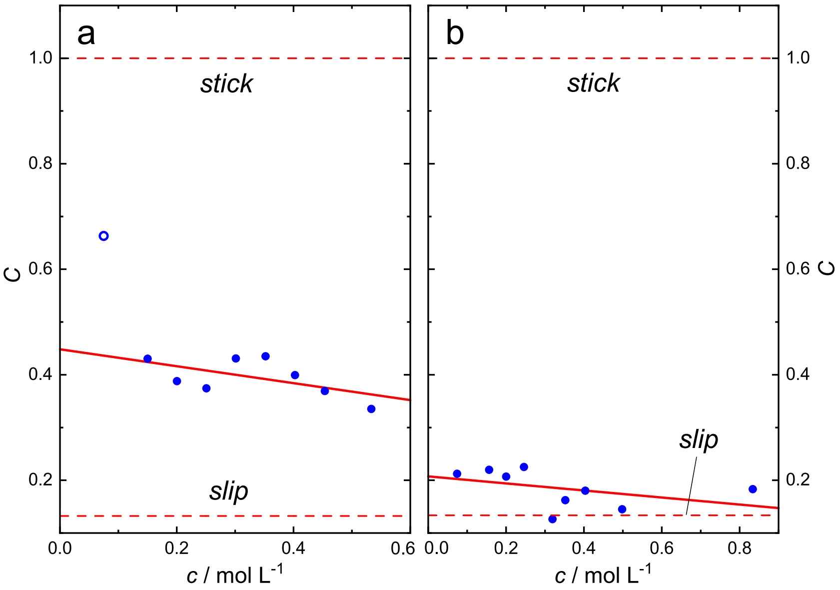

Figure S11: Hydrodynamic friction coefficients, C (●), for the rotation of (a) ACh$^+$ and (b) CCh$^+$ dipoles and their linear fits (solid lines; open symbols not included). Also included are the theoretical limits (broken lines) for C under *slip* or *stick* boundary conditions.

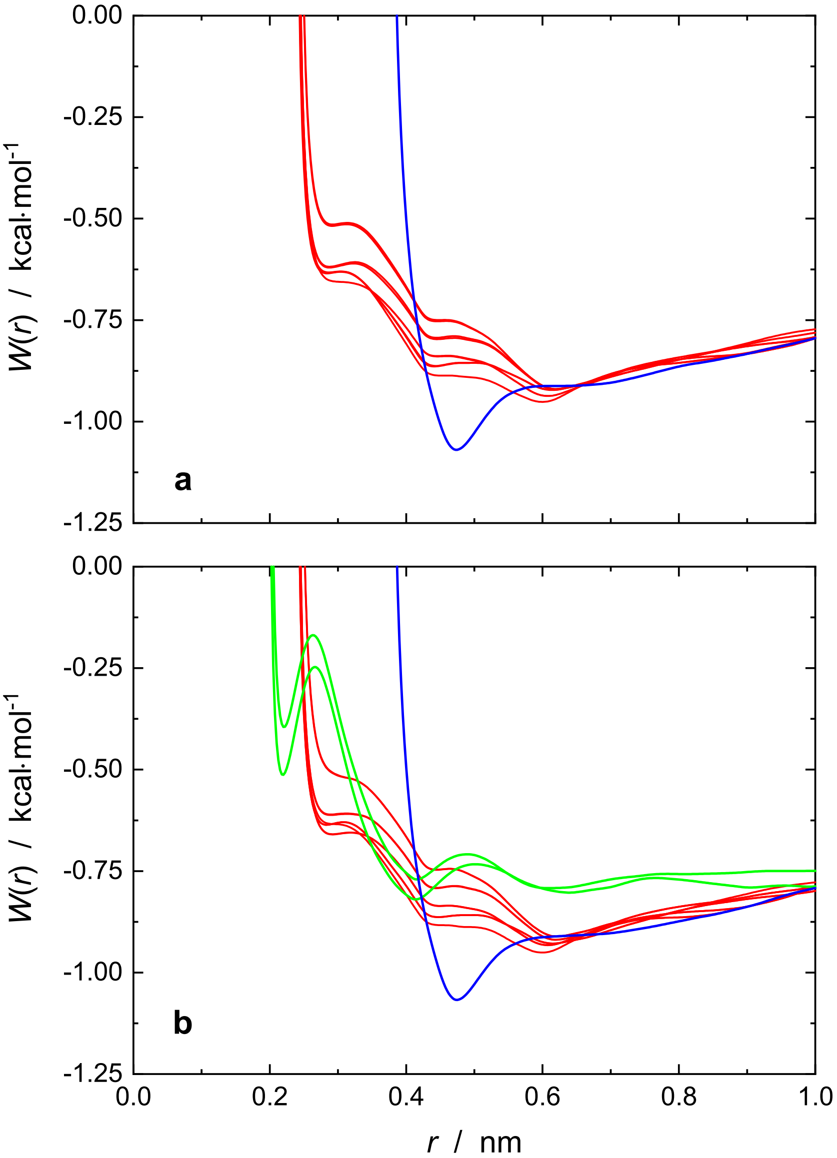

Figure S12: (a) Potentials of mean force between Cl$^-$ and the hydrogen atoms, Hm (red lines), respectively the nitrogen atom, N (blue line), of the ammonium moiety of ACh$^+$ at infinite dilution in aqueous solution. (b) Corresponding PMFs for CCh$^+$(aq) (same colour code). Here additionally the PMFs between Cl$^-$ and the hydrogen atoms, Ha, of the carbamoyl moiety are shown (gree lines). For atom labelling see Fig. 1 of the Main Manuscript.

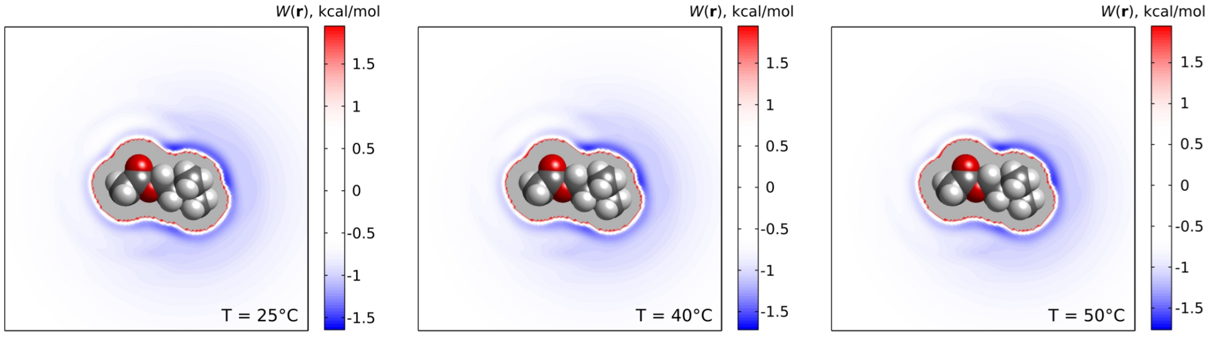

a *b* *c*

Figure S13: 2D-maps of the potential of mean force between cation and anion for *TT* AChCl obtained from 3D-RISM at 25 °C (a), 40 °C (b) and 50 °C (c).

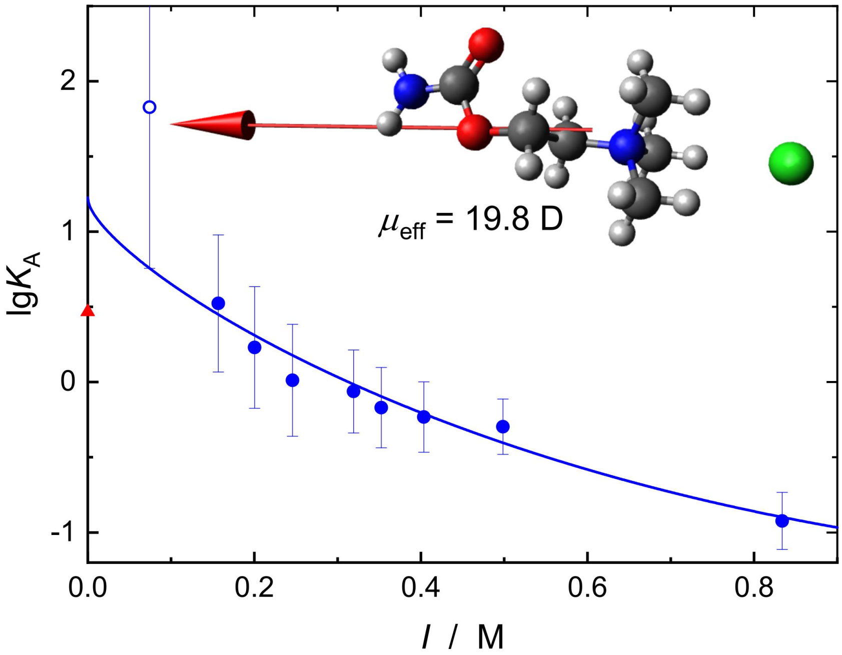

Figure S14: Association number, K_{A} (●), as a function of nominal ionic strength, I, calculated from the ion-pair amplitude, S_0, of CChCl(aq) and assuming a linear CIP with TT-CCh$^+$ (see insert). The line shows the corresponding Guggenheim-type fit (open symbol not included). Also shown is the standard-state association constant from conductivity, K_{A}° (▲).

References

[1] M. Bešter-Rogač and D. Habe, *Acta Chim. Slov.*, 2006, **53**, 391–395.

[2] *CRC-Handbook of Chemistry and Physics*, ed. D. R. Lide, CRC-Press, Boca Raton, USA, 85th edn., 2004.

[3] J. M. G. Barthel, H. Krienke and W. Kunz, *Physical Chemistry of Electrolyte Solutions-Modern Aspects*, Steinkopff, Springer, Darmstadt, New York, 1998.

[4] M. Bešter-Rogač, R. Neueder and J. Barthel, *J. Solution Chem.*, 1999, **28**, 1071–1086.

[5] Y. Marcus, *Ion Properties*, Wiley, Chichester, 1997.

[6] H. S. Harned and B. B. Owen, *The Physical Chemistry of Electrolyte Solutions*, Reinhold, New York, 1958.

[7] J. Barthel, R. Buchner, P. N. Eberspächer, M. Münsterer, J. Stauber and B. Wurm, *J. Mol. Liq.*, 1998, **78**, 83–109.

[8] T. Sonnleitner, D. A. Turton, S. Waselikowski, J. Hunger, A. Stoppa, M. Walther, K. Wynne and R. Buchner, *J. Mol. Liq.*, 2014, **192**, 19–25.

[9] S. Schrödle, G. Hefter, W. Kunz and R. Buchner, *Langmuir*, 2006, **22**, 924–932.

[10] T. Sonnleitner, D. A. Turton, G. Hefter, A. Ortner, S. Waselikowski, M. Walther, K. Wynne and R. Buchner, *J. Phys. Chem. B*, 2015, **119**, 8826–8841.

[11] F. Kremer and A. Schönhals, *Broadband Dielectric Spectroscopy*, Springer, Berlin, 2002.

[12] A. Stoppa, A. Nazet, R. Buchner, A. Thoman and M. Walther, *J. Mol. Liq.*, 2015, **212**, 963–968.

[13] A. Eiberweiser, A. Nazet, G. Hefter and R. Buchner, *J. Phys. Chem. B*, 2015, **119**, 5270–5281.

[14] G. Chang, W. C. Guida and W. C. Still, *J. Am. Chem. Soc.*, 1989, **111**, 4379–4386.

[15] A. Bochevarov, E. Harder, T. Hughes, J. Greenwood, D. Braden, D. Philipp, D. Rinaldo, M. Halls, J. Zhang and R. Friesner, *Int. J. Quantum Chem.*, 2013, **18**, 2110–2142.

[16] D. J. Tannor, B. Marten, R. Murphy, R. A. Friesner, D. Sitkoff, A. Nicholls, M. Ringnalda, W. A. Goddard III and B. Honig, *J. Am. Chem. Soc.*, 1994, **116**, 11875–11882.

[17] B. Marten, K. Kim, R. A. Cortis, C. Friesner, R. Murphy, M. Ringnalda, D. Sitkoff and B. Honig, *J. Phys. Chem.*, 1996, **100**, 11775–11788.

[18] Schrödinger, LLC, New York, NY, USA, *Jaguar, Release 2017-3*, 2017.

[19] D. Chandler and H. C. Andersen, *J. Chem. Phys.*, 1972, **57**, 1930–1937.

[20] A. Kovalenko and F. Hirata, *J. Chem. Phys.*, 2000, **113**, 2793–2805.

[21] A. Kovalenko, in *Three-dimensional RISM theory for molecular liquids and solid-liquid interfaces*, ed. F. Hirata, Kluwer, Dordrecht, 2003, pp. 169–276.

[22] A. Kovalenko and F. Hirata, *J. Chem. Phys.*, 1999, **110**, 10095–10112.

[23] J. Wang, R. M. Wolf, J. W. Caldwell, P. A. Kollman and D. A. Case, *J. Comput. Chem.*, 2004, **25**, 1157–1174.

[24] L. Lue and D. Blankschtein, *J. Phys. Chem.*, 1992, **92**, 8582–8594.

[25] S. R. Cox and D. E. Williams, *J. Comput. Chem.*, 1981, **2**, 304–323.

[26] D. A. Case, R. M. Betz, W. Botello-Smith, D. S. Cerutti, T. E. Cheatham III, T. A. Darden, R. E. Duke, T. J. Giese, H. Gohlke, A. W. Goetz, N. Homeyer, S. Izadi, P. Janowski, J. Kaus, A. Kovalenko, T. S. Lee, S. LeGrand, P. Li, C. Lin, T. Luchko, R. Luo, B. Madej, D. Mermelstein, K. M. Merz, G. Monard, H. Nguyen, H. T. Nguyen, I. Omelyan, A. Onufriev, D. R. Roe, A. Roitberg, C. Sagui, C. L. Simmerling, J. Swails, R. C. Walker, J. Wang, R. M. Wolf, X. Wu, L. Xiao, D. M. York and P. A. Kollman, *AMBER 2016*, University of California: San Francisco, 2016.

[27] A. Kovalenko, S. Ten-no and F. Hirata, *J. Comput. Chem.*, 1999, **20**, 928–936.

[28] S. B. Brummer and G. J. Hills, *Trans. Faraday Soc.*, 1961, **57**, 1823–1837.

[29] J. L. Dote and D. Kivelson, *J. Phys. Chem.*, 1983, **87**, 3889–3893.

[30] C. F. J. Böttcher and P. Bordewijk, *Theory of Electric Polarization, Vol. 2*, Elsevier, Amsterdam, 1978.

[31] J. F. Zemaitis, D. Cark, M. Rafal and N. C. Scrivner, *Handbook of Aqueous Electrolyte Thermodynamics: Theory & Application*, Wiley-AIChE, Hoboken, New Jersey, 1986.

[32] A. Y. Zasetzky and R. Buchner, *J. Phys.: Condens. Matter*, 2011, **23**, 025903.

[33] V. Balos, S. Imoto, R. R. Netz, M. Bonn, D. J. Bonthuis, Y. Nagata and J. Hunger, *Nature Commun.*, 2020, **11**, 1611.

[34] M. V. Fedotova, S. E. Kruchinin and G. N. Chuev, *J. Mol. Liq.*, 2020, **304**, 112757.